Parasitol Res (2015) 114:2873–2881
DOI 10.1007/s00436-015-4488-x

ORIGINAL PAPER

Trypanosoma cruzi infection and benznidazole therapy independently stimulate oxidative status and structural pathological remodeling of the liver tissue in mice

Rômulo Dias Novaes[1,2,4] · Eliziária C. Santos[3] · Marli C. Cupertino[3] · Daniel S. S. Bastos[3] · Jerusa M. Oliveira[3] · Thaís V. Carvalho[3] · Mariana M. Neves[3] · Leandro L. Oliveira[3] · André Talvani[2,4]

Received: 10 March 2015 / Accepted: 16 April 2015 / Published online: 28 April 2015

Abstract This study used a murine model of Chagas disease to investigate the isolated and combined impact of *Trypanosoma cruzi* infection and benznidazole (BZ) therapy on liver structure and function. Male C57BL/6 mice were challenged with *T. cruzi* and BZ for 15 days. Serum levels of cytokines and hepatic enzymes, liver oxidative stress, morphology, collagen, and glycogen content were monitored. Separately, *T. cruzi* infection and BZ treatment resulted in a pro-oxidant status and hepatic reactive damage. Concurrently, both *T. cruzi* infection and BZ treatment induced upregulation of antioxidant enzymes and pathological reorganization of the liver parenchyma and stroma. *T. cruzi* infection increased serum levels of Th1 cytokines, which were reduced by BZ in both infected and non-infected animals. BZ also induced functional organ damage, increasing serum levels of liver enzymes. When combined, *T. cruzi* infection and BZ therapy elicited intense hepatic reactive damage that was not compensated by antioxidant enzymatic reaction, subsequently culminating in more severe morphofunctional hepatic injury. Taken together, these findings indicate that during specific treatment of Chagas disease, hepatic pathology may be a result of an interaction between BZ metabolism and specific mechanisms activated during the natural course of *T. cruzi* infection, rather than an isolated toxic effect of BZ on liver structure and function.

Keywords Chagas disease · Morphology · Oxidative stress · Pathology · Protozoan parasite

✉ Rômulo Dias Novaes
romuonovaes@yahoo.com.br

[1] Department of Structural Biology, Federal University of Alfenas, Alfenas 37130-000, Minas Gerais, Brazil

[2] Department of Biological Sciences and NUPEB, Federal University of Ouro Preto, Ouro Preto 35400-000, Minas Gerais, Brazil

[3] Department of General Biology, Federal University of Viçosa, Viçosa 36570-000, Minas Gerais, Brazil

[4] Laboratório de Imunobiologia da Inflamação DECBI/NUPEB, Universidade Federal de Ouro Preto, Ouro Preto 35400-000, MG, Brazil

Introduction

The current therapeutic management of Chagas disease, a systemic disease caused by *Trypanosoma cruzi* infection in vertebrate hosts, is limited to etiological treatment based on nitroheterocyclic drugs such as nifurtimox and benznidazole (BZ). Although these drugs do not cure the disease, once it reaches the chronic phase, they have a high curative rate in the early acute phase in animals and humans (Castro et al. 2006; Guedes et al. 2011).

Since the early 1960s, BZ (*N*-benzyl-2-nitroimidazole acetamide) has been the drug of choice for treatment of Chagas disease, especially in Central and South American countries (Mecca et al. 2008). In the acute phase of infection by *T. cruzi*, therapeutic schemes based on BZ have been widely accepted; however, clinical studies have reported marked side effects associated with low specificity and systemic toxicity, as evidenced by clinical manifestations such as vomiting, fever, skin allergies, anorexia, polyneuritis, and reduced bone marrow cell production (Castro et al. 2006; Maya et al. 2010; Urbina 2010).

Evidence suggests that the toxic effect of BZ involves enzymatic reduction of the nitro group attached to the aromatic ring present in the chemical structure of the drug. This enzymatic reduction is responsible for covalent modifications of the host macromolecules in a process mediated by the

cytochrome P450 reductase enzymatic complex (Rodrigues Coura and De Castro 2002; Castro et al. 2006; Maya et al. 2007; Urbina 2010). Enzymatic processing of BZ leads to the formation of reactive intermediates such as nitro anion radical ($R\text{-}NO^{2-}$), and its re-oxidation results in the formation of reactive oxygen species (ROS) and reactive nitrogen species (RNS) (Maya et al. 2007; Urbina 2010; Esperandim et al. 2013). This process synthesizes electrophilic compounds such as hydroxylamine and nitrosative derivatives, which increase the toxicity of BZ against both the parasite and the host cells (Castro et al. 2006; Maya et al. 2007). The biotransformation of BZ by the enzymatic complex of hepatic microsomes has been reported to have a strong relationship with alterations of liver mitochondrial functionality, which may potentially be related to the toxic nature of BZ (Rendon 2014).

Considering that systemic toxicity attributed to chemotherapeutic management of Chagas disease frequently culminates in therapy suspension, it is surprising that to date there have been few studies investigating the separate effects of *T. cruzi* infection and BZ therapy on liver tissue (Pupulin et al. 2005; Davies et al. 2014; Esperandim et al. 2013; Rendon 2014). In addition to the difficulty of determining how the infection and BZ therapy separately contribute to hepatic dysfunction, the scarcity of data relative to liver structure and function during natural evolution of *T. cruzi* infection and BZ therapy hinders the development of therapeutic strategies to improve tolerance to treatment. This study was designed to elucidate the mechanisms of toxicity associated with chemotherapy against Chagas disease by investigating the isolated and combined effects of *T. cruzi* infection and BZ therapy on morphofunctional hepatic adaptations in mice.

Materials and methods

Animals and ethics

Ten-week-old male C57BL/6 mice were obtained from the Central Animal Laboratory of the Center of Biosciences and Health of the Federal University of Viçosa (Brazil) and maintained under conditions of controlled temperature at 21±2 °C, relative humidity of 60–70 %, and 12 h light/dark cycle. The animals received food and water ad libitum. All institutional and national guidelines for the care and use of laboratory animals were followed and the study was approved by the Ethics Committee of Animal Use of the Federal University of Viçosa, Brazil (CEUA/UFV protocol 77/2012).

Treatment and parasitemia

The animals were randomized into four groups of nine animals each: non-infected (NI); non-infected and treated with 100 mg/kg BZ (NI+BZ); infected but not treated (INF); or infected and treated with 100 mg/kg BZ (INF+BZ). Infected animals were inoculated intraperitoneally (i.p.) with *T. cruzi* Y strain (5,000 trypomastigote forms in 0.1 mL of infected mouse blood). BZ (Laboratório Farmacêutico do Estado de Pernambuco, Brazil) was suspended in 1 % carboxymethyl cellulose dissolved in distilled water and administered by gavage (Caldas et al. 2008). All treatments were administered for 15 days, and the parasitaemia was determined daily from a 5 μL blood sample obtained from the tail according to Brener (1962). The animals were euthanized 24 h after the last treatment by deep anesthesia (ketamine 45 mg/kg and xylazine 5 mg/kg, i.p.), followed by cardiac puncture. The liver was collected and weighed, and the hepatosomatic index (HSI, %) was calculated by normalizing the liver weight to the final body weight.

Nitric oxide analysis

Fragments of the liver tissue were removed and weighed. Nitric oxide (NO) levels were indirectly quantified by the standard Griess reaction (Tsikas 2007). Briefly, 50 μL of supernatant from the liver homogenate was incubated with an equal volume of Griess reagent (1 % sulfanilamide, 0.1 % naphthylene diamine dihydrochloride, and 2.5 % phosphoric acid) at room temperature for 10 min. The absorbance was measured at 550 nm in a microplate scanning spectrophotometer (Power Wave X; Bio-Tek Instruments Inc., Winooski, VT, USA). The total protein content in the liver tissue was measured using the Bradford method (Bradford 1976).

Lipid and protein oxidation

For analysis of tissue malondialdehyde (MDA), an end product of lipid peroxidation, samples of the liver tissue were homogenized in phosphate buffer, centrifuged at 10,000×*g* for 10 min, and the homogenate was reacted with thiobarbituric acid solution (15 % trichloacetic acid, 0.375 % thiobarbituric acid, and 0.25 N HCl) for 15 min. The formation of thiobarbituric acid reactive substances was monitored in a spectrophotometer at 535 nm, as described previously (Buege and Aust 1978).

The protein carbonyl (PCN) content was determined in liver tissue pellets by adding 0.5 mL of 10 mM 2,4-dinitrophenylhydrazine (DNPH). The reaction involved derivatization of the carbonyl group with DNPH, which leads to the formation of a stable 2,4-dinitrophenyl hydrazone product. The optical density (OD) was measured in a spectrophotometer at 370 nm (Levine et al. 1990).

Antioxidant enzymes

The activity of antioxidant enzymes was investigated using an aliquot of frozen liver tissue (100 mg) homogenized in ice-

cold phosphate buffer (pH 7.0) and centrifuged at 3,500×*g* (5 °C) for 15 min. The supernatant was used for the analysis of catalase (CAT) and glutathione *S*-transferase (GST). CAT activity was evaluated according to the method described by Aebi (1984) by measuring the kinetics of hydrogen peroxide (H_2O_2) decomposition. GST activity was estimated spectrophotometrically at 340 nm as described by Habig et al. (1974) and calculated from the rate of NADPH oxidation. Superoxide dismutase (SOD) activity was estimated by a xanthine oxidase method based on the production of H_2O_2 and the reduction of nitroblue tetrazolium (Sarban et al. 2005).

Functional markers of hepatic damage

Blood samples were centrifuged at 3,000×*g* for 15 min. Serum was collected and aspartate aminotransferase (AST), alanine aminotransferase (ALT), and alkaline phosphatase (ALP) were quantified using commercial enzymatic kits (Bioclin Laboratories, Belo Horizonte, MG, Brazil) and used as functional biomarkers of hepatic damage (Amacher 1998; Bissel et al. 2001; Novaes et al. 2012).

Enzyme-linked immunosorbent assay (ELISA) for cytokines

Serum samples were collected for cytokine assays. The concentrations of cytokines were measured by sandwich ELISA. The chemokine ligand 2 (CCL2, or MCP-1), tumor necrosis factor-alpha (TNF-α), interferon gamma (IFN-γ), and interleukin (IL)-10 were measured using commercial kits as per the manufacturer's instructions (Uscn Life Science Inc., Wuhan, China). Briefly, equal volumes of serum and 1.2 % trifluoroacetic acid/1.35 M NaCl were mixed and left at room temperature for 10 min. The samples were then centrifuged for 5 min at 3,000×*g* and supernatants adjusted for salt content (0.14 M sodium chloride and 0.1 M sodium phosphate) and pH 7.4 for determination of the concentrations of soluble cytokines. All samples were measured simultaneously in duplicate.

Histopathology and stereology

Fragments of liver tissue (median lobe) were removed and immediately immersed in freshly prepared histological fixative (10 % formaldehyde in 0.1 M phosphate buffer *w/v*, pH 7.2) for 48 h at room temperature for morphological analysis (Novaes et al. 2013). The fixed fragments were dehydrated in ethanol, cleared in xylol, and embedded in paraffin. Blocks were cut into 4-μm-thick histological sections and stained with hematoxylin–eosin (H&E) for general histopathology and 4′,6-diamidino-2-phenylindole (DAPI) for DNA. To avoid repetitive analysis of the same histological area, sections were evaluated in semi-series using one in every 20 sections. The slides were visualized with a 40× objective lens, and images were captured using a light microscope (Olympus BX-60; Tokyo, Japan) equipped with a digital camera (Olympus QColor-3; Tokyo, Japan) (Novaes et al. 2012, 2013).

A stereological method was used to determine volume density (Vv, %) of liver components (sinusoid capillaries, interstitium, hepatocytes, hepatocyte nuclei, and interstitial cell nuclei). The volume density was calculated using the formula: $Vv=P_P/P_T$, where P_P is the number of test points located on the structure of interest and P_T is the total test points in the histological area (Novaes et al. 2012). These parameters were measured in ten histological fields per animal at 400× magnification using sections stained with H&E, Sirius Red, DAPI, and by the Best's Carmine method for glycogen and a test system with 300 test points in the standard test area of 73×10^3 μm^2 at the tissue level. All stereological and morphological analysis was performed using Image Pro-Plus 4.5 image analysis software (Media Cybernetics, Silver Spring, MD, USA).

Glycogen and collagen analysis

Glycogen was extracted according to the method described by Hassid and Abrahams (1957). Briefly, fresh liver samples (50 mg) were digested by heating (100 °C) in 0.5 mL of 5 N KOH for 60 min. Glycogen was purified and precipitated by 99 % ethanol in boiling water and then centrifuged at 8,000×*g* for 20 min. The pellets obtained were resuspended in distilled water (1 mL) and 3 ml of anthrone solution (50 mg diluted in 50 mL of 84 % H_2SO_4) and incubated for 10 min at 100 °C. The OD was measured at 620 nm (Power Wave X).

For each experimental group, 35 8-μm-thick histological sections stained with Fast Green and Sirius Red (Mobay Chemical Co., Union, NJ, USA) were used to quantify the levels of collagen and total protein in scar tissue using a previously described spectrophotometric method (López-De León and Rojkind 1985). In this method, the maximal absorbance to the Sirius Red (540 nm) and Fast Green (605 nm) dyes correspond to the amount of collagen and non-collagen proteins, respectively.

Statistical analysis

The results were expressed as mean±standard deviation. Parametric data were compared with Student's *t* test and nonparametric data were compared with the Mann–Whitney *U* test. Statistical significance was established at $p<0.05$. All tests were performed using the GraphPad Prism 5.01 statistical software (GraphPad Software Inc., San Diego, CA, USA).

Results

The mean parasitemia of infected and non-treated animals was significantly higher compared with the group receiving BZ. While blood parasitism was maintained in infected and non-treated animals, blood of mice treated with BZ was 100 % clear of parasite at the end of the experimental period (data not shown). The liver mass and hepatosomatic index of infected animals treated with BZ were significantly greater than the other groups (Table 1).

Separately, *T. cruzi* infection or BZ exposure increased hepatic reactive stress compared with control non-infected animals (Fig. 1). *T. cruzi* infection alone was not sufficient to induce protein oxidation. In general, the infection and BZ therapy interacted to increase the liver content of NO and MDA compared with the other groups ($p<0.001$). *T. cruzi* infection and BZ treatment independently increased the activity of hepatic antioxidant enzymes compared with control animals. Infected animals presented reduced activity of CAT and SOD compared with animals exposed to BZ ($p<0.001$; Fig. 2).

The quantification of circulating cytokines indicated that BZ treatment alone acted on the immune system reducing the TNF-α and IFN-γ serum levels, which were drastically increased by *T. cruzi* infection compared to control animals. IL-6 levels were similar in infected animals treated with BZ and the control group. However, TNF-α and IFN-γ levels were significantly reduced in infected animals treated with BZ compared with non-treated animals (Fig. 3).

In the infected animals and both groups receiving BZ, serum biochemical analysis indicated functional evidence of hepatocyte injury, represented by high serum levels of the hepatic enzymes ALT and AST compared with the control group ($p<0.001$). The levels of these enzymes were significantly higher in the groups exposed to BZ compared with the infected and non-treated group ($p<0.001$; Fig. 4).

Parasitized cells were not identified in liver tissue. Separately, *T. cruzi* infection or BZ therapy modified liver microscopic structure. Histopathological changes in liver tissue were more pronounced in both groups receiving BZ (especially in animals that were both infected and treated), and the more obvious changes were reduction of cytoplasm granularity, hepatocyte hypertrophy, obliteration of sinusoidal spaces, and attenuation of nucleolar staining. Stereological analysis revealed that *T. cruzi* infection or BZ treatment alone, and in particular, the combination of both, reduced volume density of sinusoid capillaries and interstitial space, and increased tissue density of hepatocytes compared with the control group ($p<0.001$; Fig. 5). Epifluorescence microscopy showed marked reduction in volume density of hepatocyte nuclei in both infected animals and those exposed to BZ compared with control animals ($p<0.001$). This reduction was most evident in infected animals receiving BZ treatment. Infected and non-treated animals presented higher cellularity of interstitial cells compared with the other groups ($p<0.05$). Increased relation between hepatocytes and interstitial cell nuclei was observed in infected animals and those treated with BZ compared with control animals. BZ therapy did not aggravate this relation in infected animals (Fig. 6). Glycogen content in the liver tissue was reduced only in infected, non-treated animals compared with the other groups ($p<0.05$). The collagen content was similar in all groups (Fig. 7).

Discussion

Although BZ-based chemotherapy remains as the reference therapeutic approach for Chagas disease, understanding of the mechanisms underlying the poor organic tolerability of anti-*T. cruzi* chemotherapy is still fragile (Pupulin et al. 2005; Rendon 2014). In this study to investigate the impact of *T. cruzi* infection and BZ therapy on liver function and structure, mice were infected with the Y strain of *T. cruzi* because the strain is partially resistant to BZ and induces high parasitemia (Bahia et al. 2012). BZ was administered at 100 mg/kg, a reference dose used in preclinical studies (Caldas et al. 2008; Diniz et al. 2013). There is evidence that lower doses have low efficacy against *T. cruzi*, while larger

Table 1 Mean parasitemia, biometric parameters, and food intake in response to *T. cruzi* infection and benznidazole (BZ) therapy in mice

Parameters	NI	NI+BZ	INF	INF+BZ
MP, 0.1 mL blood×10^3	ND	ND	21.60±8.84a	8.82±1.46b
Initial body mass, g	24.17±3.72a	23.35±3.96a	24.09±3.75a	23.38±3.06a
Final body mass, g	25.92±2.85a	24.27±3.11a	22.18±3.62a	23.51±3.19a
Liver mass, g	1.11±0.15a	1.25±0.21a,b	1.19±0.19a,b	1.40±0.17b
HSI, %	4.28±1.16a	5.15±1.42a	5.37±1.22a	5.96±1.12b
MFI, g/day	6.91±0.39a	6.60±0.52a	5.01±0.43b	6.37±0.51a

Different letters (a, b) denote statistical difference among the groups ($p<0.05$)

MP mean parasitemia, *ND* non-detected, *HSI* hepatosomatic index, *MFI* mean food intake, *NI* non-infected animals, *NI+BZ* non-infected treated with 100 mg/kg BZ, *INF* infected non-treated, *INF+BZ* infected treated with 100 mg/kg BZ

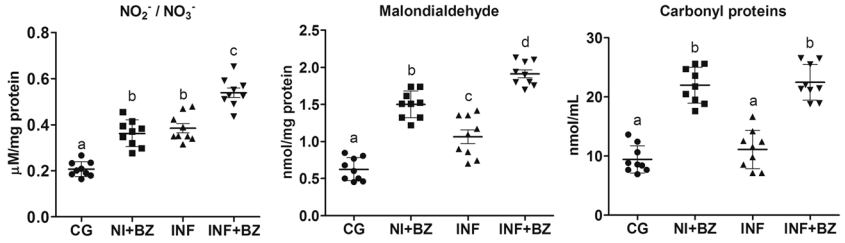

Fig. 1 Hepatic reactive damage in response to *T. cruzi* infection and benznidazole (*BZ*) therapy in C57BL/6 mice. *MDA*, malondialdehyde; *PCN*, carbonyl protein. *NI*, non-infected animals; *NI+BZ*, non-infected treated with 100 mg/kg BZ; *INF*, infected non-treated; *INF+BZ*, infected treated with 100 mg/kg BZ. *a*, *b*, *c*, *d* Different *letters* denote statistical difference among the groups, $p<0.05$

doses have high toxicity in the host without significant contribution to therapeutic outcomes (Cançado 2002; Castro et al. 2006; Guedes et al. 2011).

In this study, *T. cruzi* infection and BZ exposure separately resulted in marked oxidative damage to lipids and proteins in the liver tissue. Furthermore, *T. cruzi* infection and BZ therapy interacted to increase the hepatic pro-oxidant status and resulted in more severe reactive damage. RNS and ROS production have been implicated in BZ toxicity (Castro et al. 2006; Urbina 2010; Esperandim et al. 2013). Clinically, these metabolites have been associated with poor organic tolerability during BZ exposure, constituting potential therapeutic targets in adjuvant therapies to counteract BZ toxicity (Maya et al. 2007; Urbina 2010; Guedes et al. 2011). The production of RNS (especially NO) and ROS (particularly OH^{-}, $O_2^{\bullet-}$, and H_2O_2) has been indicated as an important trypanocidal mechanism of the host (Nagajyothi et al. 2012; Wen et al. 2014) and is also responsible for a significant portion of BZ activity against *T. cruzi* (Maya et al. 2010; Guedes et al. 2011). There is evidence that, during the natural course of *T. cruzi* infection, ROS production is primarily mediated by the respiratory burst in activated leukocytes in an attempt to destroy circulating parasites and abnormal parasitized cells (Pérez-Fuentes et al. 2003; Bergeron and Olivier 2006; Gupta et al. 2009). Reinforcing host defenses, NO (a pivotal molecule against *T. cruzi*) synthesis is enhanced by upregulation of immune-mediated iNOS (inducible NO synthase), activating nitrosative processes against *T. cruzi* and host tissues (Bergeron and Olivier 2006; Gupta et al. 2009; Nagajyothi et al. 2012; Wen et al. 2014). Conversely, by inducing NO production, BZ also triggers a nitrosative process, an event that is apparently independent of the conventional enzymatic mechanisms associated with NO synthase. Evidence indicates that NO is produced by a direct pathway during BZ metabolism, specifically through direct reduction of the nitro group in the molecule chain by nitroreductase enzymes (Castro et al. 2006; Urbina 2010). This process is not isolated and has been described as a coupled reaction in which one-electron reduction results in the formation of the nitro anion radical, and its re-oxidation determines the synthesis of radical and non-radical ROS that act together with NO against parasitic infection (Castro et al. 2006; Maya et al. 2007; Guedes et al. 2011). However, this process generates unstable nitroso- and hydroxylamine intermediates, which, due to low specificity and cross-reactions with host biomolecules, induce the formation of drug–protein/drug–thiol conjugates and cause single-strand breaks in DNA, alkylation of proteins, and lipid peroxidation (Rodrigues Coura and De Castro 2002; Castro et al. 2006). Lipid peroxidation, a pathological process that plays a pivotal role in liver damage due to its autocatalytic characteristics, was clearly observed in the present study (i.e., MDA). Previous studies have indicated that oxidation of unsaturated fatty acids in the hepatocyte membranes determines the production of lipid peroxyl radicals (LOO^{-}), alkoxy radicals (RO^{-}), and MDA, which propagates oxidative damage in the cyclic process of lipid oxidation (Kappus 1987; Gonçalves et al. 2012; Novaes et al. 2012).

In addition to reactive tissue damage, the activity of hepatic antioxidant enzymes was independently increased in infected animals and those exposed to BZ. There is evidence that tolerance to drugs whose toxic effects are mediated by reactive metabolites is dependent on organic antioxidant status (Sagara

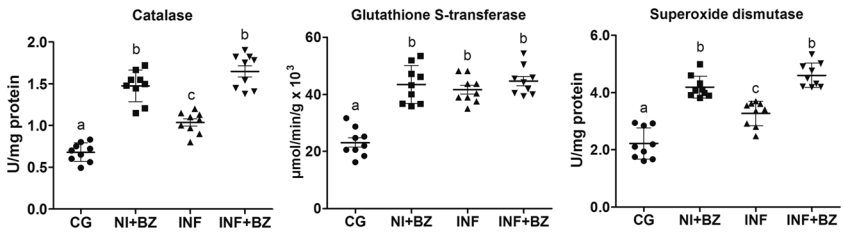

Fig. 2 Activity of hepatic antioxidant enzymes in response to *T. cruzi* infection and benznidazole (BZ) therapy in C57BL/6 mice. *CAT*, catalase; *GST*, glutathione *S*-transferase; *SOD*, superoxide dismutase. *NI*, non-infected animals; *NI+BZ*, non-infected treated with 100 mg/kg BZ; *INF*, infected non-treated; *INF+BZ*, infected treated with 100 mg/kg BZ. *a*, *b*, *c* Different *letters* denote statistical difference among the groups, $p<0.05$

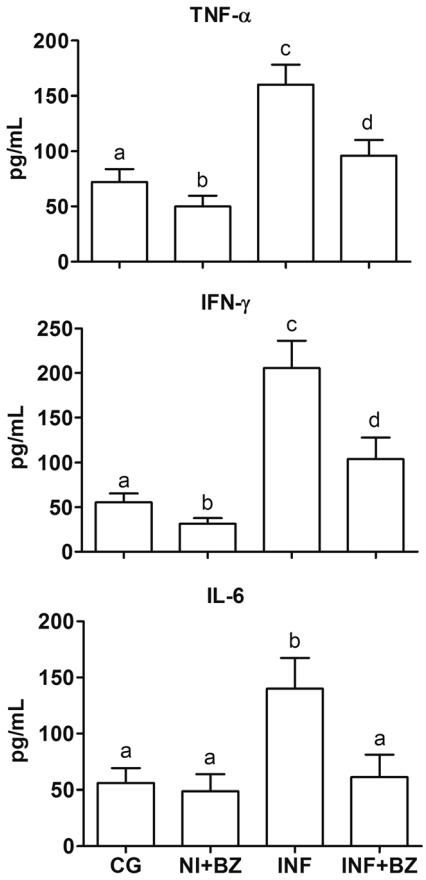

Fig. 3 Serum levels of cytokines in response to *T. cruzi* infection and benznidazole (BZ) therapy in C57BL/6 mice. *NI*, non-infected animals; *NI+BZ*, non-infected treated with 100 mg/kg BZ; INF, infected non-treated; *INF+BZ*, infected treated with 100 mg/kg BZ. *a*, *b*, *c*, *d* Different *letters* denote statistical difference among the groups, $p<0.05$

et al. 1998; Bissel et al. 2001; Lee 2003; Cupertino et al. 2013). Enzymatic antioxidant processes are particularly well developed in liver tissue, blocking, or attenuating reactive damage during drug metabolism (Bissel et al. 2001; Lee 2003; Cupertino et al. 2013). Thus, SOD catalyzes dismutation of $O_2^{\bullet-}$ to O_2 and H_2O_2 and represents the first line of enzymatic defense against ROS. CAT, by decomposing H_2O_2 in water and molecular oxygen, plays a major role in protecting cells against reactive damage. In addition, by catalyzing the conjugation of glutathione with multiple reactive species, GST (a phase II enzyme of drug biotransformation) also presents remarkable scavenging potential (Sagara et al. 1998; Pedrosa et al. 2001). In the present study, both *T. cruzi* infection and BZ therapy independently challenged the hepatic antioxidant system, causing an enzymatic readjustment to counteract nitrosative and oxidative stresses and to minimize reactive tissue damage. This modulatory mechanism was clearly dependent on the nature of the challenge, being more intense in reaction to BZ exposure than to *T. cruzi* infection.

BZ exposure resulted in high ALT and AST serum levels, evidence of increased membrane instability and permeability in hepatocytes (Amacher 1998; Ozer et al. 2008; Gonçalves et al. 2012; Cupertino et al. 2013). This finding indicated that BZ therapy, but not *T. cruzi* infection alone, overpowered the hepatic antioxidant mechanisms that are required to maintain hepatocyte integrity against reactive damage. The different hepatic functional repercussions of BZ therapy and *T. cruzi* infection can be partially attributed to specific mechanisms by which reactive stress is activated in each condition. High levels of reactive metabolites are generated directly during BZ metabolism (Rodrigues Coura and De Castro 2002; Castro et al. 2006; Maya et al. 2007; Urbina 2010), but, with *T. cruzi* infection, the generation of reactive metabolites is indirect and regulated by immunological mediators such as cytokines in a process called inflammatory oxidative stress (Gupta et al. 2009; Nagajyothi et al. 2012; Wen et al. 2014). In fact, in the present study, the proportion of interstitial cells (i.e., inflammatory cells) in liver tissue, and circulating levels of IFN-γ, TNF-α, and IL-6 were drastically increased by infection and reduced by BZ, which indicated potential to reduce pro-inflammatory cytokines even in the absence of infection (i.e., group NI+BZ). Beyond participating in parasite control, these cytokines also directly stimulate the synthesis of reactive species by leukocytes, disrupting the tissue redox balance, and favoring reactive tissue damage (Pérez-Fuentes et al. 2003; Bergeron and Olivier 2006; Gupta et al. 2009; Nagajyothi et al. 2012).

In addition to functional damage, *T. cruzi* infection and BZ exposure caused pathological reorganization of the liver

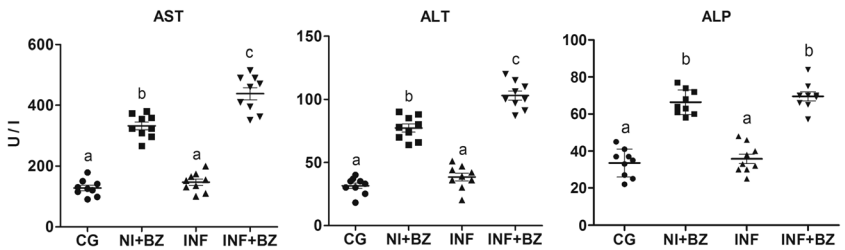

Fig. 4 Serum levels of hepatic enzymes in response to *T. cruzi* infection and benznidazole (BZ) therapy in C57BL/6 mice. *AST*, aspartate aminotransferase; *ALT*, alanine aminotransferase; *ALP*, alkaline phosphatase. *NI*, non-infected animals; *NI+BZ*, non-infected treated with 100 mg/kg BZ; *INF*, infected non-treated; *INF+BZ*, infected treated with 100 mg/kg BZ. *a*, *b*, *c*, *d* Different *letters* denote statistical difference among the groups, $p<0.05$

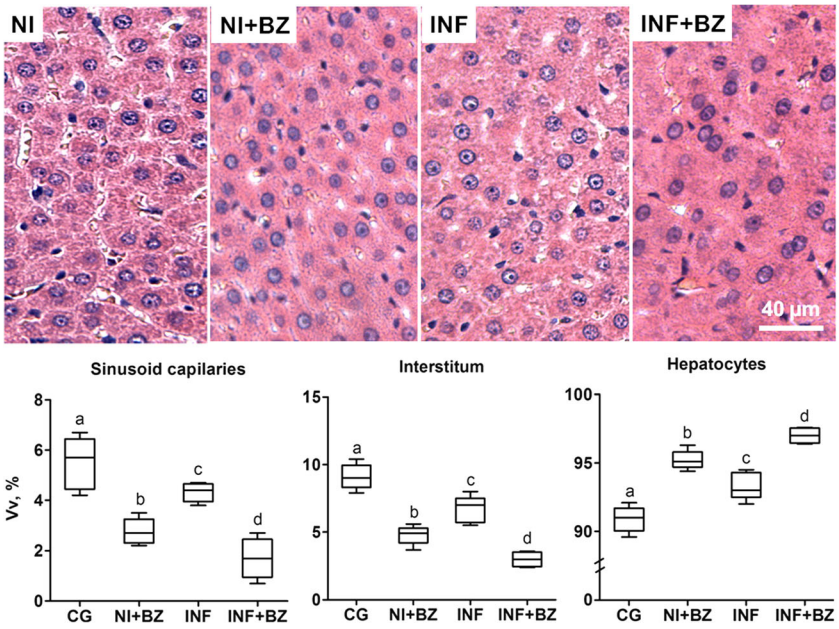

Fig. 5 Representative photomicrographs and stereological parameters of parenchymal and stromal components of the liver tissue in response to *T. cruzi* infection and benznidazole (BZ) therapy in C57BL/6 mice (H&E staining under bright field microscopy, *bars*=40 μm for all images). *NI*, non-infected animals; *NI+BZ*, non-infected treated with 100 mg/kg BZ; *INF*, infected non-treated; *INF+BZ*, infected treated with 100 mg/kg BZ. *Vv*, volume density. The *graphs* show the results of stereological analysis. *a*, *b*, *c*, *d* Different *letters* denote statistical difference among the groups, $p<0.05$

stroma and parenchyma. Although collagen content was similar in all groups, *T. cruzi* infection alone reduced hepatic glycogen content, a condition potentially related to reduced food intake due to organic debility from infection and high energy expenditure typical of systemic infections. In general, more severe histopathological findings were observed in infected animals receiving BZ, in which microscopic evidence of interstitial compression (i.e., Vv of sinusoid capillaries and interstitium) and increased volume density and reduced nuclei density of hepatocytes, indicated cellular hypertrophy.

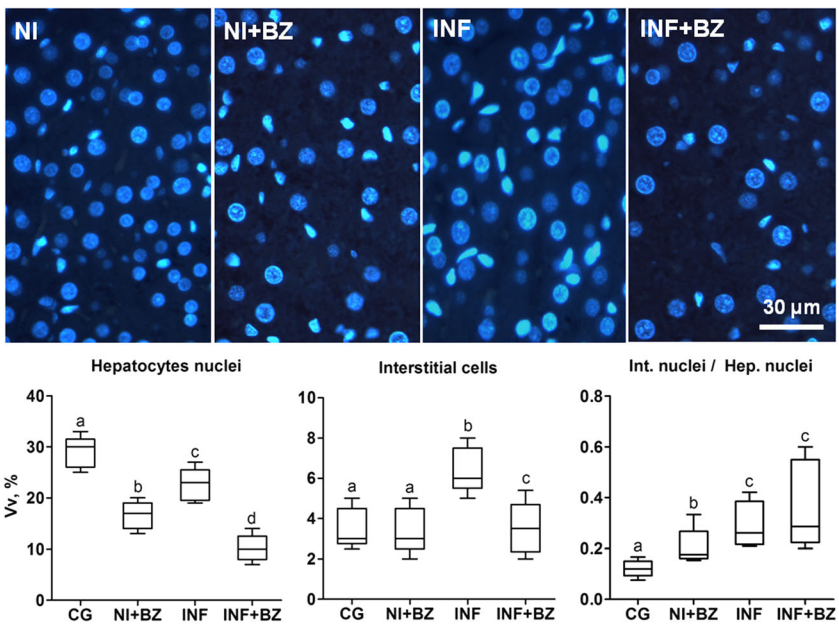

Fig. 6 Representative photomicrographs and cellularity of the liver tissue in response to *T. cruzi* infection and benznidazole (BZ) therapy in C57BL/6 mice (DAPI staining under epifluorescence microscopy, *bar*= 30 μm for all images). *NI*, non-infected animals; *NI+BZ*, non-infected treated with 100 mg/kg BZ; *INF*, infected non-treated; *INF+BZ*, infected treated with 100 mg/kg BZ. The *graphs* show the results of stereological analysis. *Vv*, volume density; *Int*, interstitium; *Hep*, hepatocytes. *a*, *b*, *c*, *d* Different *letters* denote statistical difference among the groups, $p<0.05$

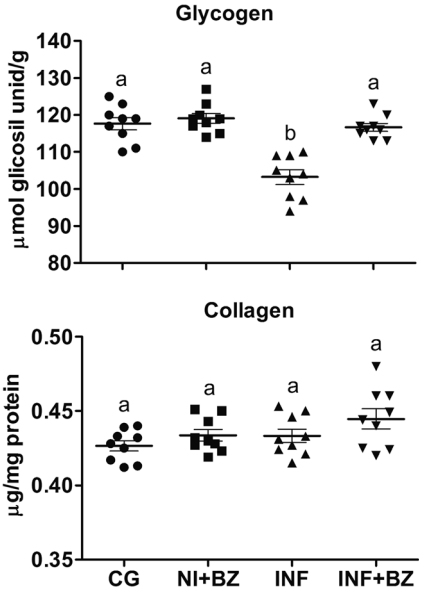

Fig. 7 Glycogen and collagen content in the liver tissue in response to *T. cruzi* infection and benznidazole (BZ) therapy in C57BL/6 mice. *NI*, non-infected animals; *NI+BZ*, non-infected treated with 100 mg/kg BZ; *INF*, infected non-treated; *INF+BZ*, infected treated with 100 mg/kg BZ. *a*, *b*, *c*, *d* Different *letters* denote statistical difference among the groups, $p<0.05$

Beyond these histopathological changes, increased liver mass and hepatosomatic index indicated that infection and BZ therapy also interacted to induce liver hypertrophy. Frequently, reports of BZ toxicity are accompanied by inconsistencies such as absence of biometric, structural, ultrastructural, or mitochondrial deleterious effects after drug exposure (Mecca et al. 2008; Esperandim et al. 2013; Rendon 2014). Considering the different methodological approaches, it is possible that this finding is influenced by multiple factors such as time of treatment, differential susceptibility to *T. cruzi* infection, and variable patterns of resistance to BZ therapy in the different models investigated. In fact, very little evidence suggests different levels of tolerance to BZ in target organs. Apparently, the liver is more susceptible to injury than the heart, an issue that remains unclear but is probably related to BZ metabolism, distribution, and efficiency of defense mechanisms in specific organs (Harris 1992; Sagara et al. 1998; Esperandim et al. 2013) and refractory tissues (Mecca et al. 2008; Rendon 2014). Although *T. cruzi* infection provides a morphofunctional insult to liver tissue, BZ treatment offers an even greater challenge to hepatic antioxidant defense mechanisms, which frequently fail to neutralize large amounts of reactive metabolites, accumulating reactive molecular damage that can contribute to the poor organic tolerability associated with anti-*T. cruzi* chemotherapy.

In conclusion, this study indicated that both *T. cruzi* infection and BZ therapy are separately able to induce systemic and hepatic pathological adaptations, modulating circulating levels of cytokines, inducing hepatic lipid and protein oxidation, upregulating antioxidant enzyme activity, and determining marked morphological reorganization of the liver parenchyma and stroma. When combined, *T. cruzi* infection and BZ therapy increased the severity of hepatic injury, possibly related to nitrosative and oxidative stress triggered by specific mechanisms activated during the natural course of infection and BZ metabolism. Thus, this evidence supports the hypothesis that hepatic pathology observed during treatment of Chagas disease could be the result of an interaction between infection and BZ chemotherapy, rather than an isolated effect of BZ treatment on liver structure and function.

Acknowledgments The authors would like to acknowledge the "Fundação de Amparo a Pesquisa do Estado de Minas Gerais - FAPEMIG" and "Conselho Nacional de Desenvolvimento Científico e Tecnológico - CNPq". André Talvani is CNPq fellow.

Conflict of interest The authors declare that they have no conflict of interest.

Ethical approval All applicable international, national, and institutional guidelines for the care and use of animals were followed.

References

Aebi H (1984) Catalase in vitro. Methods Enzymol 105:121–126

Amacher DE (1998) Serum transaminase elevations as indicators of hepatic injury following the administration of drugs. Regul Toxicol Pharmacol 27:119–130

Bahia MT, de Andrade IM, Martins TA, do Nascimento ÁF, Diniz LF, Caldas IS, Talvani A, Trunz BB, Torreele E, Ribeiro I (2012) Fexinidazole: a potential new drug candidate for Chagas disease. PLoS Negl Trop Dis 6, e1870

Bergeron M, Olivier M (2006) *Trypanosoma cruzi*-mediated IFN-γ-inducible nitric oxide output in macrophages is regulated by iNOS mRNA stability. J Immunol 177:6271–6280

Bissel DM, Gores GJ, Laskin DL, Hoofnagle JH (2001) Drug-induced liver injury: mechanisms and test systems. Hepatology 33:1009–1013

Bradford MM (1976) A rapid and sensitive method for the quantitation of microgram quantities of protein utilizing the principle of protein-dye-binding. Anal Biochem 7:248–254

Brener Z (1962) Therapeutic activity and criterion of cure on mice experimentally infected with *Trypanosoma cruzi*. Rev Inst Med Trop Sao Paulo 4:389–396

Buege JA, Aust SD (1978) Microsomal lipid peroxidation. Methods Enzymol 52:302–310

Caldas IS, Talvani A, Caldas S, Carneiro CM, De Lana M, Da Matta Guedes PM, Bahia MT (2008) Benznidazole therapy during acute phase of Chagas disease reduces parasite load but does not prevent chronic cardiac lesions. Parasitol Res 103:413–421

Cançado JR (2002) Long term evaluation of etiological treatment of chagas disease with benznidazole. Rev Inst Med Trop Sao Paulo 44:29–37

Castro JA, De Mecca MM, Bartel LC (2006) Toxic side effects of drugs used to treat Chagas' disease (American trypanosomiasis). Hum Exp Toxicol 25:471–479

Cupertino MC, Costa KLC, Santos DCM, Novaes RD, Condessa SS, Neves AC, Oliveira JA, Matta SLP (2013) Long-lasting morphofunctional remodelling of liver parenchyma and stroma after

a single exposure to low and moderate doses of cadmium in rats. Int J Exp Pathol 94:343–351

Davies C, Dey N, Negrette OS, Parada LA, Basombrio MA, Garg NJ (2014) Hepatotoxicity in mice of a novel anti-parasite drug candidate hydroxymethylnitrofurazone: a comparison with benznidazole. PLoS Negl Trop Dis 8, e3231

Diniz LF, Urbina JA, de Andrade IM, Mazzeti AL, Martins TA, Caldas IS, Talvani A, Ribeiro I, Bahia MT (2013) Benznidazole and posaconazole in experimental Chagas disease: positive interaction in concomitant and sequential treatments. PLoS Negl Trop Dis 7, e2367

Esperandim VR, da Silva Ferreira D, Sousa Rezende KC, Cunha WR, Saraiva J, Bastos JK, Andrade E, Silva ML, de Albuquerque S (2013) In vivo infection by *Trypanosoma cruzi*: a morphometric study of tissue changes in mice. Parasitol Res 112:431–436

Gonçalves RV, Novaes RD, Leite JPV, Vilela EF, Cupertino MC, Nunes LG, Matta SLP (2012) Hepatoprotective effect of *Bathysa cuspidata* in a murine model of severe toxic liver injury. Int J Exp Pathol 93: 370–376

Guedes PM, Silva GK, Gutierrez FR, Silva JS (2011) Current status of Chagas disease chemotherapy. Expert Rev Anti Infect Ther 9:609–620

Gupta S, Wen JJ, Garg NJ (2009) Oxidative stress in Chagas disease. Interdisc Perspect Infect Dis 190354:1–8

Habig WH, Pabst MJ, Jakoby WB (1974) Glutathione *S*-transferases: the first enzymatic step in mercapturic acid formation. J Biol Chem 249: 7130–7139

Harris ED (1992) Regulation of antioxidant enzymes. FASEB J 6:2675–2683

Hassid WZ, Abraham S (1957) Chemical procedures for analisys of polyssacarides. Methods Enzymol 3:34–50

Kappus HA (1987) A survey of chemicals inducing lipid peroxidation in biological systems. Chem Phys Lipids 45:105–111

Lee WM (2003) Drug-induced hepatotoxicity. N Engl J Med 349:474–481

Levine RL, Garland D, Oliver CN, Amici A, Climent I, Lenz AG, Ahn BW, Shaltiel S, Stadtman ER (1990) Determination of carbonyl content in oxidatively modified proteins. Methods Enzymol 186: 464–478

López-De León A, Rojkind M (1985) A simple micromethod for collagen and total protein determination in formalin-fixed paraffin-embedded sections. Histochem Cytochem 33:737–743

Maya JD, Cassels BK, Iturriaga-Vásquez P, Ferreira J, Faúndez M, Galanti N, Ferreira A, Morello A (2007) Mode of action of natural and synthetic drugs against *Trypanosoma cruzi* and their interaction with the mammalian host. Comp Biochem Physiol A Mol Integr Physiol 146:601–620

Maya JD, Orellana M, Ferreira J, Kemmerling U, López-Muñoz R, Morello A (2010) Chagas disease: present status of pathogenic mechanisms and chemotherapy. Biol Res 43:323–331

Mecca MM, Bartel LC, Castro CR, Castro JÁ (2008) Benznidazole biotransformation in rat heart microsomal fraction without observable ultrastructural alterations: comparison to Nifurtimox-induced cardiac effects. Mem Inst Oswaldo Cruz 103:549–553

Nagajyothi F, Zhao D, Weiss LM, Tanowitz HB (2012) Curcumin treatment provides protection against *Trypanosoma cruzi* infection. Parasitol Res 110:2491–2499

Novaes RD, Gonçalves RV, Marques DC, Cupertino MC, Peluzio MC, Leite JP, Maldonado IR (2012) Effect of bark extract of *Bathysa cuspidata* on hepatic oxidative damage and blood glucose kinetics in rats exposed to paraquat. Toxicol Pathol 40:62–70

Novaes RD, Penitente AR, Gonçalves RV, Talvani A, Peluzio MC, Neves CA, Natali AJ, Maldonado IR (2013) *Trypanosoma cruzi* infection induces morphological reorganization of the myocardium parenchyma and stroma, and modifies the mechanical properties of atrial and ventricular cardiomyocytes in rats. Cardiovasc Pathol 22:270–279

Ozer J, Ratner M, Shaw M, Bailey W, Schomaker S (2008) The current state of serum biomarkers of hepatotoxicity. Toxicology 245:194–205

Pedrosa RC, De Bem AF, Locatelli C, Pedrosa RC, Geremias R, Wilhelm Filho D (2001) Time-dependent oxidative stress caused by benznidazole. Redox Rep 6:265–270

Pérez-Fuentes R, Guégan J-F, Barnabé C, López-Colombo A, Salgado-Rosas H, Torres-Rasgado E, Briones B, Romero-Díaz M, Ramos-Jiménez J, Sánchez-Guillén Mdel C (2003) Severity of chronic Chagas disease is associated with cytokine/antioxidant imbalance in chronically individuals. Int J Parasitol 33:293–299

Pupulin ART, Paludetto A, da Silva SV, Bracht AMK (2005) Benznidazol effects in perfunded rat liver. RBAC 37:153–156

Rendon D (2014) Alterations of mitochondria in liver but not in heart homogenates after treatment of rats with benznidazole. Hum Exp Toxicol 33:1066–1070

Rodrigues Coura J, De Castro SL (2002) A critical review on Chagas disease chemotherapy. Mem Inst Oswaldo Cruz 97:3–24

Sagara Y, Dargusch R, Chambers D, Davis J, Schubert D, Maher P (1998) Cellular mechanisms of resistance to chronic oxidative stress. Free Radic Biol Med 24:1375–1389

Sarban S, Kocyigit A, Yazar M, Isikan UE (2005) Plasma total antioxidant capacity, lipid peroxidation, and erythrocyte antioxidant enzyme activities in patients with rheumatoid arthritis and osteoarthritis. Clin Biochem 38:981–986

Tsikas D (2007) Analysis of nitrite and nitrate in biological fluids by assays based on the Griess reaction: appraisal of the Griess reaction in the L-arginine/nitric oxide area of research. J Chromatogr B Analyt Technol Biomed Life Sci 15:51–70

Urbina JA (2010) Specific chemotherapy of Chagas disease: relevance, current limitations and new approaches. Acta Trop 115:55–68

Wen JJ, Nagajyothi F, Machado FS, Weiss LM, Scherer PE, Tanowitz HB, Garg NJ (2014) Markers of oxidative stress in adipose tissue during *Trypanosoma cruzi* infection. Parasitol Res 113:3159–3165